

Olefin Polymerization Behavior of Titanium(IV) Pyridine-2-phenolate-6-(σ -aryl) Catalysts: Impact of “py-Adjacent” and Phenolate Substituents

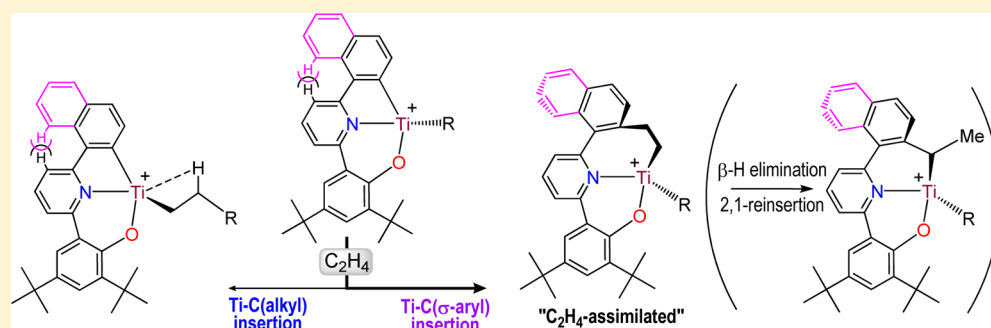
Jerry C. Y. Lo,[†] Michael C. W. Chan,^{*,†} Po-Kam Lo,[†] Kai-Chung Lau,^{*,†} Takashi Ochiai,[§] and Haruyuki Makio[‡]

[†]Department of Biology and Chemistry, City University of Hong Kong, Tat Chee Avenue, Kowloon, Hong Kong, People's Republic of China

[§]R&D Center, Mitsui Chemicals, Inc., 580-32 Nagaura, Sodegaura, Chiba 299-0265, Japan

[‡]Mitsui Chemicals Singapore R&D Centre Pte. Ltd., 50 Science Park Road, #06-08 The Kendall Singapore Science Park II, Singapore 117406

S Supporting Information



ABSTRACT: A series of Ti(IV) post-metallocene bis(benzyl) precatalysts supported by tridentate pyridine-2-phenolate-6-(σ -aryl) [O,N,C] ligands, featuring various substituents on the σ -aryl (directly adjacent to the pyridine ring: fluoro, trifluoromethyl, benzo [C₄H₄]) and phenolate groups (*tert*-butyl, trifluoromethyl, cumyl, 1,1-diphenylethyl), have been prepared. Multinuclear (including ¹H, ¹³C, and ¹⁹F) NMR characterizations of the complexes have been performed. The principal purpose of this study was to investigate the impact of these substituents upon ethylene polymerization reactivity and polymer properties. The cumyl-phenolate σ -naphthyl Ti precatalyst, in conjunction with [Ph₃C][B(C₆F₅)₄], displays good activity and produces polyethylene with exceptionally high MW ($M_n = 4 \times 10^6$) and an M_w/M_n value (2.5) approaching single-site character at 50 °C, but multisite behavior is apparent for other catalysts. DFT calculations have been performed to probe the polymerization behavior and the role of the py-adjacent substituent. These studies revealed the possibility of two distinct polymerization reactions, namely conventional and ethylene-assimilated (comprising initial ethylene insertion into the Ti–C(σ -aryl) bond) chain propagation, and found that the latter is kinetically preferred. Furthermore, the viability of another kinetically competitive pathway, namely the isomerization of the ethylene-assimilated [Ti–CH₂CH₂–aryl] species via β -H elimination and 2,1-reinsertion, was also indicated.

INTRODUCTION

Amongst a myriad of multidentate ancillary ligands, chelating σ -aryl auxiliaries have increasingly gained prominence in postmetallocene catalyst design for olefin polymerization.¹ Priced by studies on non-Cp (cyclopentadienyl) carbon-based anionic ligands,² zirconium complexes with tridentate bis(σ -aryl)amine ligands were developed as precatalysts for propylene polymerization, but low efficiency and broad molecular weight distribution were reported.³ Therein, Hessen noted that aromatic σ -carbanions are principally σ -donors with minimal π -donation (in contrast to amide and phenolate moieties) and can potentially confer a more electrophilic metal center. However, a critical caveat is that the M–C(sp²) bond must be inert relative to the M–C(sp³) bond, which would generally be true especially in the absence of steric effects,

and the study concluded by recognizing the possibility of competitive insertion into the respective Zr–C(aryl) and Zr–C(alkyl/polymeryl) bonds.³ Indeed, the feasibility of olefin insertion into the M–C(sp²) bond of a chelating σ -aryl ligand was subsequently demonstrated by the facile, stoichiometric reactivity toward ethylene or propylene of a cationic titanium bis(phenolate) complex supported by a bidentate (σ -aryl)amine ligand.⁴ Intramolecular ortho-metalation processes mediated by group 4 derivatives bearing aryl-substituted auxiliaries to afford chelating σ -aryl moieties have been described.^{5,6}

Researchers at Symyx and Dow developed a high-performance class of pyridylamido [N,N,C]-Hf(IV) catalysts containing

Received: August 29, 2012

Published: January 10, 2013

ortho-metalated phenyl and naphthyl substituents for olefin polymerization through the use of high-throughput screening, which produce isotactic polypropylene materials with extremely high molecular weights.⁷ Intriguingly, ethylene-(α -olefin) copolymers from these catalysts display broad, multimodal molecular weight distributions (MWD), indicative of multisite behavior, and a mechanism involving monomer insertion into the Hf–C(σ -naphthyl) bond was proposed to rationalize this, on the basis of evidence from DFT calculations, ¹³C NMR and GC/MS analysis, and isolation of olefin-inserted products.⁸ For propylene polymerization, DFT calculations revealed that monomer insertion into the Hf–C(σ -aryl) bond can generate multiple active species with different reactivities, consistent with the observed multimodal MWD.⁹ Coates reported living 1-hexene and unexpected isotactic propylene polymerizations using a C_s-symmetry (σ -phenyl)pyridylamido Hf catalyst.¹⁰ Extensive NMR studies were performed by Macchioni to investigate the activation of [N,N,C]-Hf precatalysts.¹¹ Notably, Brønsted acids protonate the σ -naphthyl moiety to afford a Hf $\cdots\eta^2$ -naphthyl interaction, driven presumably by the release of an eclipsed H \cdots H repulsion between the naphthyl and pyridyl units, which corresponds to that proposed to account for the favorable monomer-inserted mechanism.⁸ Furthermore, detailed NMR experiments supported by DFT calculations were undertaken to probe the viability of α -olefin insertion into the Hf–C(σ -aryl) bond and characterize the resultant species, and evidence was presented which indicates that such catalytic sites are significantly more active than conventional “noninserted” species.¹² The observation of both diastereomers arising from rotation of the 2-isopropylphenyl unit in the ligand backbone of [N,N,C]-Hf and -Zr precatalysts and a comparison of their ethylene-(1-octene) and propylene polymerization characteristics were described.¹³ For analogous Zr derivatives bearing a σ -phenyl, -furyl, or -thienyl moiety, an additional species, formed by metalation of an isopropyl group on the amido moiety, was identified from aged catalyst solutions and proposed to be the active site responsible for producing high- M_n materials.¹⁴

Inspired by the monomer-inserted mechanism to develop ligand frameworks featuring an ancillary C(sp³) donor, a pyridylamido ligand bearing a pendant vinyl unit was prepared, which was found to undergo intramolecular vinyl insertion into a neutral Hf(IV) trimethyl complex to generate a living isoselective propylene polymerization precatalyst containing the [Hf–CH(Et)–naphthyl] moiety.¹⁵ Similarly, metalation of a vinyl-appended phenolate-amine ligand with Zr- and Hf(CH₂Ph)₄ was accompanied by benzyl migration to afford complexes bearing the corresponding tridentate ligand incorporating a C(sp³) donor, which catalyze living, isoselective polymerization of α -olefins.¹⁶ The application of chelating (σ -aryl)-imine-amido Hf complexes to mediate the direct coupling of internal alkynes and 2-alkylpyridine was recently reported.¹⁷

We initially developed a family of pyridine-2-phenolate-6-(σ -aryl) [O,N,C] group 4 precatalysts bearing fluorinated substituents adjacent to the metal center,¹⁸ and evidence from multinuclear NMR spectroscopy suggesting the existence of intramolecular C–H \cdots F–C contacts was supported by a neutron diffraction study.¹⁹ These complexes constitute synthetic models of weak attractive ligand–polymer interactions in olefin polymerization,²⁰ and it is significant to note that recent reports concerning late transition metal systems hint at the generality of this concept for modulating polymerization reactions.^{21,22} Investigations into the impact of σ -aryl substituents upon olefin homo- and copolymerizations by Ti precatalysts, in conjunction

with MAO and trityl borate,^{23,24} revealed that (1) a substituent adjacent to the metal center is not essential and can adversely affect efficiency, (2) a “py-adjacent” σ -aryl substituent (Cl, Me, benzo (C₆H₄)), in an ortho position directly adjacent to the pyridyl ring, can improve polymerization activities, and (3) broad MWD polymers are produced, implying multisite behavior. Bearing in mind the highly rigid nature of [O,N,C] ligands, and a crystal structure that contains an eclipsed interaction between a py-adjacent chloro substituent and the relevant pyridyl proton, we hypothesized that the seemingly remote py-adjacent substituent may affect the conformation of the M–ligand chelation and destabilize the Ti–C(σ -aryl) linkage, thereby facilitating olefin insertion into this bond to afford supplementary olefin-assimilated²⁵ active species with enhanced efficiencies, like that reported for the [N,N,C]-Hf system.^{7–13} In this context, systems displaying remote or indirect substituent effects in olefin polymerization have been described in the literature,²⁶ while the conformational consequences of the bridging moiety in *ansa*-metallocenes upon polymerization reactivity are well-established.²⁷ Several reports on highly active Cp-based and post-metallocene catalysts for olefin polymerization have recently appeared.²⁸

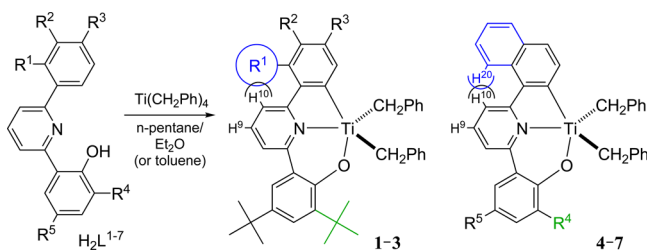
Our objectives are to develop greater understanding of substituent effects in the Ti-[O,N,C] system, derive insight into the olefin polymerization mechanism(s) for improved catalyst design and performance, and produce narrow-MWD polymers while also investigating the multisite characteristics of the polymerization process and the nature of these active species. We have evaluated the impact of changing both phenolate and py-adjacent substituents, as well as steric and electronic factors, upon polymerization behavior. The observed polymerization results are rationalized with the aid of DFT calculations, which provide insight into different reaction pathways and the generation and reactivity of the postulated olefin-assimilated active species, and possible explanations for the superior efficiencies of σ -naphthyl catalysts. Comparisons with the (σ -aryl)pyridylamido Hf system are also made. The cumyl-phenolate σ -naphthyl Ti precatalyst, in conjunction with [Ph₃C][B(C₆F₅)₄], produces exceptionally high MW polyethylene ($M_n = 4 \times 10^6$; $M_w/M_n = 2.5$; activity = 2.7 kg mmol⁻¹ h⁻¹) at 50 °C.

■ RESULTS AND DISCUSSION

Synthesis and NMR Characterization. The pyridine-2-phenolate-6-(σ -aryl) ligands were synthesized by modification of literature procedures that entail the sequential coupling of two substituted acetophenones, while taking advantage of the synthetic accessibility (for trifluoromethyl, cumyl, and 1,1-diphenylethyl derivatives) and commercial availability of substituted acetophenones (see the Supporting Information for details).^{29,30} Cyclometalations of ligands H₂L^{1–7} with Ti(CH₂Ph)₄ were performed in a diethyl ether/*n*-pentane or toluene/*n*-pentane mixture at –78 °C and allowed to proceed upon warming to 20 °C for 12 h. The titanium complexes (Scheme 1) were obtained as dark red crystalline solids in moderate to good isolated yields (40–78%), except for 6 and 7 (ca. 28%); this is partially ascribed to their high solubility in nonpolar solvents.

All complexes have been fully characterized by ¹H (plus ¹⁹F) and ¹³C NMR spectroscopy and assigned using 135-DEPT, [¹H,¹H]-COSY, [¹³C,¹H]-HSQC, and ROESY experiments (plus [¹H,¹⁹F]-HMQC for 3). A salient point of interest is the impact of the py-adjacent substituent (R¹) upon the pyridyl group, as indicated by the respective ¹H NMR shifts for the pyridyl hydrogens H^{9,10} (Table 1). For both 1 and 2, the

Scheme 1. Synthesis of Complexes 1–7



H ₂ L ⁿ	R ¹	R ²	R ³	R ⁴	R ⁵	complex
H ₂ L ¹	F	H	H	^t Bu	^t Bu	1
H ₂ L ²	F	H	F	^t Bu	^t Bu	2
H ₂ L ³	CF ₃	H	H	^t Bu	^t Bu	3
H ₂ L ⁴	benzo (C ₆ H ₄)	H	H	^t Bu	^t Bu	4
H ₂ L ⁵	benzo (C ₆ H ₄)	H	CF ₃	H	H	5
H ₂ L ⁶	benzo (C ₆ H ₄)	H	CMe ₂ Ph	Me	H	6
H ₂ L ⁷	benzo (C ₆ H ₄)	H	CPh ₂ Me	H	H	7

Table 1. Influence of py-Adjacent Substituent (R¹) upon ¹H NMR Shifts^a for H^{9,10}

complex	R ¹	H ¹⁰ (ppm)	H ⁹ (ppm)	Δδ(H ^{9,10})	R ¹ /H ¹⁰ interaction
1	F	7.60	6.73	0.87	J _{H,F} = 2.9 Hz
2	F	7.46	6.73	0.73	J _{H,F} = 2.6 Hz
3	CF ₃	7.25	6.73	0.52	[¹ H, ¹⁹ F]-HMQC
4	benzo	7.12	6.73	0.39	NOE (with H ²⁰)
5	benzo	7.09	6.67	0.42	NOE (with H ²⁰)
6	benzo	7.01	6.64	0.37	NOE (with H ²⁰)
7	benzo	7.04	6.64	0.40	NOE (with H ²⁰)

^aConditions: C₆D₆, 400 MHz, 298 K. See Scheme 1 for labeling.

magnitude of the observed ¹⁹F coupling for H¹⁰ is consistent with ¹J_{H,F} (rather than ⁵J_{H,F}) and suggests weak attraction.¹⁹ However, ¹⁹F coupling with the CF₃ group is not discernible for H¹⁰ in the ¹H NMR spectrum of 3, although some correlation is apparent in the more sensitive [¹H,¹⁹F]-HMQC spectrum. Exchange peaks observed in ROESY NMR experiments between H¹⁰ and H²⁰ (in the benzo moiety) in complexes 4–7 confirm their proximity. Differences in Δδ(H^{9,10}) values may be tentatively ascribed to the varying extent of interaction (attractive or repulsive) between R¹ and H¹⁰. In contrast to the benzo group in 4, the capability of the CF₃ group in 3 to rotate and modulate interaction (repulsive or attractive) with H¹⁰ is noted (see DFT calculations for further discussion).

¹H and ¹³C NMR spectroscopy have been employed to evaluate the distortion and hence coordination of benzyl groups in 1–7 (Table S1 in the Supporting Information). Using criteria established in the literature,³¹ the reduced ²J_{H,H} (8.0–8.5 Hz) and high ¹J_{C,H} values (135.0–137.4 ppm) signify η² coordination of benzyl groups in all complexes. In addition, the η² coordination mode can be manifested as a high-field *o*-Ph ¹H NMR shift (6.34–6.76 ppm), although the influence of ring currents from ancillary ligands makes this criterion less reliable, and this is indeed apparent for the cumyl and 1,1-diphenylethyl derivatives. In comparison with analogous Zr (weaker η² coordination) and Hf derivatives (η¹ coordination),^{23,24} the η²-benzyl coordination for the Ti complexes cannot be rationalized

on steric grounds and reflects their greater electrophilicity, although differences between substituents are not evident. We note that all [O,N,C] complexes in which the bis(benzyl) moieties in the molecular structure protrude toward the pyridyl unit in an “anti, anti” arrangement (rather than “syn, anti”;³² Figure S1 in the Supporting Information) consistently exhibit a high-field ¹H NMR resonance for *p*-Ph (<6.50 ppm in C₆D₆),^{19,23,24} and the corresponding shifts (6.30–6.41 ppm) for 1–7 also tentatively indicate this conformation.

Olefin Polymerization Studies Using Trityl Borate Cocatalyst. The complexes in this work have been evaluated as ethylene polymerization catalysts in conjunction with ^tBu₃Al/[Ph₃C][B(C₆F₅)₄]. Details of polymerization reactions at 50 and 100 °C and polymer characterization are given in Table 2, which show good activities for such elevated temperatures.

Table 2. Ethylene Polymerization Results^a

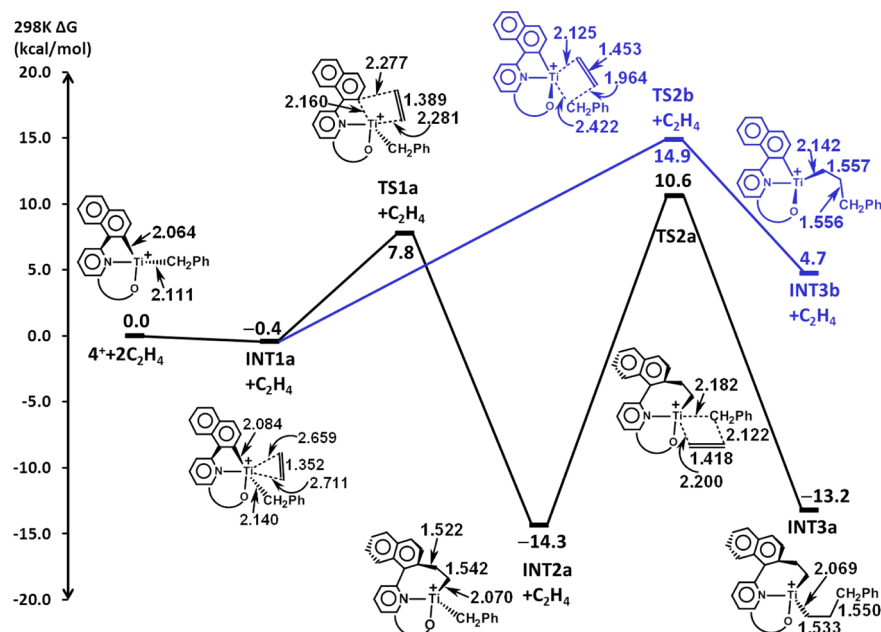
catalyst ^b	temp (°C)	yield (mg)	activity ^c	M _n (×10 ³) ^d	M _w /M _n ^d
1 (^t Bu/F)	50	111	1.1 (1.3)	1.72	2.8
	100	98	1.0 (2.1)	0.26	3.8
2 (^t Bu/2F)	50	98	1.0 (1.2)	0.87	4.9
	100	74	0.7 (1.6)	0.15	6.7
3 (^t Bu/CF ₃)	50	155	1.6 (1.9)	0.82	7.5
	100	92	0.9 (2.0)	0.06	19.2
4 (^t Bu/benzo)	50	226	2.3 (2.7)	0.41	8.1
	100	355	3.6 (7.7)	0.26	6.7
5 (CF ₃ /benzo)	50	173	1.7 (2.1)	0.57	10.8
	100	107	1.1 (2.3)	0.19	11.0
6 (CMe ₂ Ph/benzo)	50	265	2.7 (3.2)	3.99	2.5
	100	216	2.2 (4.7)	1.52	4.6
7 (CPh ₂ Me/benzo)	50	412	4.1 (4.9)	0.83	7.6
	100	229	2.3 (5.0)	0.51	14.2

^aConditions: 5 mL of toluene, 0.3 μmol of catalyst, ^tBu₃Al/[Ph₃C][B(C₆F₅)₄]/catalyst (50/2/1 equiv, respectively), 7 atm of ethylene pressure (maintained by continuous supply), 20 min reaction time. ^bPhenolate/σ-aryl substituents, respectively, are given in parentheses. ^cActivities are given in kg of polymer (mmol of catalyst)⁻¹ h⁻¹ (±10%); activities with respect to ethylene concentration (0.836 mol/L at 50 °C and 0.461 mol/L at 100 °C) are given in parentheses in kg mmol⁻¹ h⁻¹ (mol/L of ethylene)⁻¹ (±10%). ^dDetermined by GPC at 140 °C in 1,2-dichlorobenzene using polystyrene standards.

A comparison of py-adjacent substituents (1–4) reveals that the benzo derivative 4 gives the highest activities, followed by 3 at 50 °C with 1 and 2 the lowest, while the activities for 1–3 are comparable at 100 °C. We previously postulated²⁴ that the likely repulsion between the pyridyl and benzo groups would facilitate or accelerate olefin insertion into the Ti–C(σ-aryl) bond (thus alleviating the aforementioned repulsion), like that observed by Hesse^{4a} and Rothwell³³ (for a Ti–vinyl linkage) and reported for the Hf-[N,N,C] system,^{8,9,12} to afford a supplementary catalytic entity with presumably increased efficiency. Here, an in-depth evaluation of the steric and electronic effects of the py-adjacent group has been undertaken using DFT calculations (see below).

The polymers formed by 3 and 4 display broad to very broad MWD (M_w/M_n > 6.7), while complex 1 produces polyethylene with a reasonably narrow MWD (M_w/M_n = 2.8) at 50 °C. The comparable activities found for 1 and 2 (containing an additional F atom) may imply that the electrophilicities of

Scheme 2. Gibbs Free Energy Surface for Initial C_2H_4 Insertion into Ti–C(σ -aryl) (Pathway a [in black], i.e. C_2H_4 Assimilation) and Ti–C(benzyl) Bonds (Pathway b [in blue]) of 4^+ at the B97D Level using LanL2DZ (Ti) and 6-311G(d,p) (Nonmetals) Basis Sets^a



^aRelative energies at 298 K in toluene (kcal/mol) and selected interatomic distances (Å) are given; note that Ti \cdots C_{ipso} interactions are observed in INT1a, TS1a, INT2a, TS2b, and INT3b.

the respective Ti centers are not dissimilar, since enhanced electrophilicity at an active site would typically promote olefin binding and activation for insertion, possibly leading to increased catalytic activity. The employment of fluorinated moieties as electron-withdrawing substituents is an appealing design approach.³⁴

The σ -naphthyl moiety proved to be the most active among 1–4 and was employed to evaluate the impact of the phenolate substituent (5–7) upon polymerization characteristics. This was motivated by the reported beneficial effects of an increasingly bulky phenolate substituent upon the performance of bis(phenoxyimine) group 4 catalysts.³⁵ The highest efficiency of 4.1 kg mmol⁻¹ h⁻¹ at 50 °C is recorded for 1,1-diphenylethyl (7), although the broad MWD ($M_w/M_n = 7.6$) implies the presence of multiple active sites. The polyethylene produced by the cumyl derivative 6 at 50 °C ($M_n = 3.99 \times 10^6$; $M_w/M_n = 2.5$; activity = 2.7 kg mmol⁻¹ h⁻¹) is noteworthy, with exceptionally high MW and relatively narrow MWD, implying close to single-site character (see Figure S2 in the Supporting Information for GPC traces). Conversely, complex 5 exhibits the lowest activities and very broad MWD even at 50 °C, signifying that the steric and possibly electron-withdrawing effects of the CF₃ substituent at the phenolate moiety are detrimental to the performance.

Broadening of MWD and increases in M_w/M_n values indicative of enhanced multisite behavior are observed at 100 °C, particularly for 3, 5, and 7 (see below). In general, the M_n values for 1–7 decline at 100 °C, suggesting increased tendency to undergo chain termination and deactivation processes for the active sites. In this regard, greater steric protection of the catalytic center by the phenolate substituent could be beneficial, although the possibility of improved protection (for example, against chain termination) is necessarily dependent on the suitable size and positioning of said substituent. While the 1,1-diphenylethyl moiety in 7 displays

the highest activities but produces polymers with low M_n (0.83×10^6 at 50 °C), the cumyl group in 6 gives high M_n values even at 100 °C.

The nature of the active sites in these polymerizations would be of interest, and extensive attempts have been made to characterize the products upon trityl activation by NMR spectroscopy. However, the putative Ti benzyl cationic species proved to be highly unstable and could not be observed spectroscopically.³⁶ In the following section, the ethylene insertion pathways and reactivity of different catalysts were investigated and compared using DFT calculations, from which interesting insights may be derived.

Density Functional Theory Calculations. Theoretical calculations have been performed to probe the ethylene insertion and propagation processes and the feasibility of ethylene assimilation (insertion into the Ti–C(σ -aryl) bond), and our primary focus was to study the impact of the py-adjacent substituent in 1–4. The potential energy surfaces, initial ethylene insertion and propagation mechanisms, and ligand substituent effects upon polymerization behavior for the 1⁺, 2⁺, 3⁺, and 4⁺ benzyl cations (generated by trityl activation) have been investigated by DFT. The structures and energies of all molecular species have been calculated at the B97D level³⁷ with the LanL2DZ basis set³⁸ for transition metals (Ti) and the 6-311G(d,p) basis set for nonmetal atoms. The polarizable continuum model (PCM)³⁹ is used to account for solvent effects in toluene. All calculations were performed using the Gaussian 09 program package.⁴⁰

As an illustrative example, the initial ethylene insertion at 4⁺ is found to undergo two distinct reaction pathways (Scheme 2; results for 1⁺–4⁺ are given in Table S2 in the Supporting Information): (a) C_2H_4 assimilation, namely insertion into the Ti–C(σ -aryl) bond, followed by C_2H_4 insertion into the Ti–C(benzyl) bond; (b) conventional C_2H_4 insertion into the Ti–C(benzyl) bond. At the start of pathway a, ethylene

coordination occurs at 4^+ to afford a η^2 -ethylene complex (INT1a), which then undergoes C_2H_4 insertion into the Ti–C(σ -aryl) bond via a four-centered transition state (TS1a) with an energy barrier (ΔG_{298}^\ddagger) of 7.8 kcal/mol (relative to $4^+ + C_2H_4$). In TS1a, the Ti–C(σ -aryl) bond is elongated slightly from 2.084 to 2.160 Å, while the Ti–C(ethylene) distance shortens from 2.711 to 2.281 Å. The resultant stable intermediate INT2a undergoes a second C_2H_4 insertion (*anti* to the [Ti–CH₂CH₂–aryl] linkage), but on this occasion into the Ti–C(benzyl) bond through the four-centered TS2a, to yield the propylphenyl cation INT3a. Relative to $4^+ + 2C_2H_4$ (INT2a + C_2H_4), the second C_2H_4 insertion proceeds with an activation energy ΔG_{298}^\ddagger of 10.6 (24.9) kcal/mol, signifying that the rate-determining step for pathway a is ethylene insertion into the Ti–C(benzyl) bond.

The conventional propagation pathway b resembles the latter reaction in pathway a; C_2H_4 insertion into the Ti–C(benzyl) bond of INT1a, via the four-centered TS2b, gives the intermediate INT3b. The molecular structures of TS2b and INT3b correspond to TS2a and INT3a, respectively, except for the [Ti–CH₂CH₂–aryl] linkage throughout pathway a. Importantly, the ΔG_{298}^\ddagger value for pathway b is 14.9 kcal/mol (relative to $4^+ + C_2H_4$), which is higher than that for pathway a by 4.3 kcal/mol. Thus, reaction pathway a is found to be kinetically more favorable than b.

It should be noted that for 4^+ , there exist two conformers which differ in the relative orientations of the σ -naphthyl and phenolate moieties with respect to the central pyridine ring (this applies to all species bearing a py-adjacent substituent). Furthermore, the second C_2H_4 can insert in an *anti* (I and II) or *syn* (III and IV) manner with respect to the [Ti–CH₂CH₂–aryl] or Ti–C(σ -aryl) linkage, giving rise to a total of four conformers (I–IV) for TS2a (depicted in Figure S3 in the Supporting Information for 4^+) and TS2b, respectively. Regarding conformers I and II in pathway a, the second C_2H_4 insertion occurs *anti* to the [Ti–CH₂CH₂–aryl] linkage and the Ti–CH₂Ph interaction adopts a more linear configuration

(Ti–C–C_{ipso} = 168.5 (I) and 167.5° (II) in TS2a), while η^2 -benzyl coordination is evident in III and IV (Ti...C_{ipso} = 2.543 and 2.545 Å, respectively). Each conformer of 4^+ can undergo C_2H_4 insertions according to pathways a and b, but only the pathways with the lowest ΔG_{298}^\ddagger values for TS2a and TS2b, respectively, are shown in Scheme 2.⁴¹ Generally, conformers I and II are preferred for TS2a of $1^+–4^+$, while III and IV are more favorable for TS2b (Table 3; see the following paragraph for further discussion). With the exception of 2^+ , pathway a involving C_2H_4 assimilation requires less activation energy than the conventional pathway b. In other words, although both pathways are accessible, there is a kinetic preference for pathway a over pathway b.

For pathway a, the ΔG_{298}^\ddagger values for 3^+ and 4^+ (10.7 (I) and 10.6 kcal/mol (II), respectively) are noticeably lower than those for 1^+ and 2^+ (13.2 (II) and 14.5 kcal/mol (II), respectively). This indicates that ethylene insertion/propagation is kinetically most favorable for 3^+ and 4^+ , which is consistent with the superior ethylene polymerization efficiency for catalyst 4, and to some extent 3. This reactivity trend can be rationalized by considering the η^2 -benzyl coordination and Ti...C_{ipso} interaction (Table 4). The Ti...C_{ipso} distance in INT2a for $1^+–4^+$ follows the order 1^+ (2.481 Å) \approx 2^+ (2.478 Å) < 3^+ (2.490 Å) < 4^+ (2.507 Å), which is in line with the experimental activity order of $1 \approx 2 < 3 < 4$ for ethylene polymerization at 50 °C.⁴² Hence, a longer Ti...C_{ipso} separation in 4^+ would correspond to weaker η^2 -benzyl coordination, which could reduce the activation barrier for ethylene insertion. The Ti...C_{ipso} distances in INT1a are discernibly shorter than those in INT2a (by 0.118 (2^+) to 0.152 (4^+) Å), indicative of stronger η^2 -benzyl coordination. Since ethylene insertion into the Ti–C(benzyl) bond in TS2b *anti* to the Ti–C(σ -aryl) linkage (conformers I and II) necessitates cleavage of a stronger Ti...C_{ipso} interaction in INT1a, it follows that conformers I and II are kinetically less favorable in pathway b.

A prominent feature in pathway a for 4^+ is the exothermic formation of INT2a (–14.3 kcal/mol relative to $4^+ + C_2H_4$) after C_2H_4 assimilation via TS1a. The stability of INT2a for 4^+ may be rationalized by the removal of an eclipsed H_{py}...H_{naphthyl} repulsive interaction (2.126 Å in INT1a), which was similarly proposed to provide stabilization for the [N,N,C]-Hf system.^{8,12} It is of interest to note the changing geometry of the Ti center in pathway a; as a consequence of the greater flexibility of the modified seven-membered N,C(sp³)-chelate ring, the *mer*-like [O,N,C(σ -aryl)] is transformed into a *fac*-coordinating [O,N,C(C_2H_4 -aryl)] ligand to give a metal geometry that is noticeably closer to tetrahedral. In contrast to the steric repulsion apparent in 4^+ , the calculated H_{py}...F contacts in INT1a for $1^+–3^+$ (Table 4) are consistent with attractive interactions,^{18,19,43} as supported by the observation of the corresponding $J_{H,F}$ values in 1 and 2 (Table 1). Moreover, the potential energy surface for multiple C_2H_4 insertion and

Table 3. ΔG_{298}^\ddagger (kcal/mol) for Reaction Pathways a and b Mediated by Conformers I–IV of Species $1^+–4^+$ in Toluene at the B97D Level using LanL2DZ (Ti) and 6-311G(d,p) (Nonmetals) Basis Sets

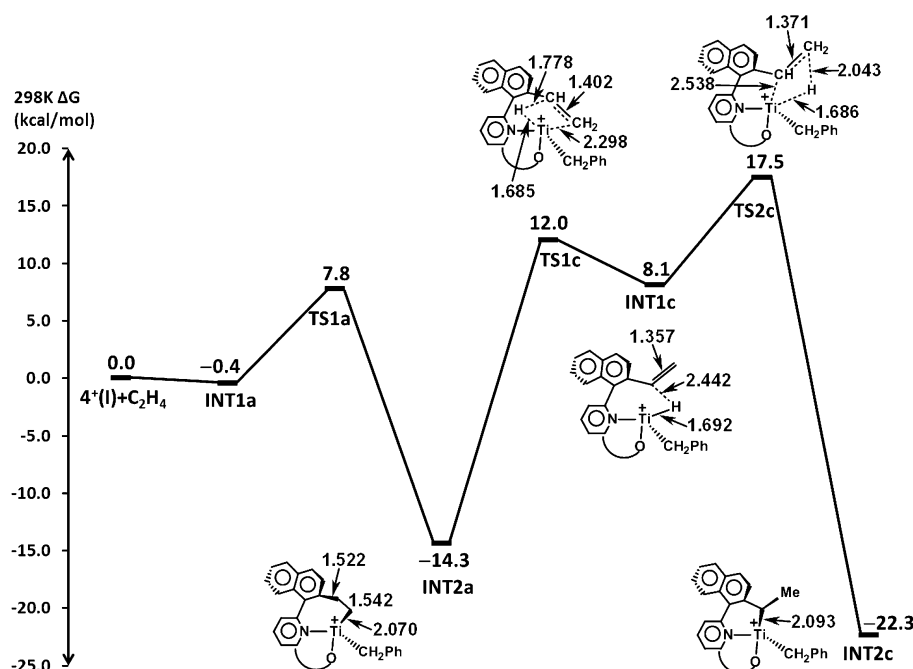
	ΔG_{298}^\ddagger							
	pathway a				pathway b			
	I	II	III	IV	I	II	III	IV
1^+	14.9	13.2	14.8	16.2	19.6	22.1	13.6	14.3
2^+	15.7	14.5	15.4	17.9	20.5	21.6	13.4	14.0
3^+	10.7	11.8	15.8	18.2	20.2	<i>a</i>	13.6	14.5
4^+	10.6	12.7	14.2	15.7	21.2	<i>a</i>	14.9	15.4

^aNot found.

Table 4. Selected Interatomic Distances and Angles for INT1a and INT2a of $1^+–4^+$ at the B97D Level using LanL2DZ (Ti) and 6-311G(d,p) (Nonmetals) Basis Sets

complex	INT1a		INT2a		INT1a: closest H _{py} ...R ¹ _{aryl} contact	
	Ti...C _{ipso} (Å)	Ti–C–C _{ipso} (deg)	Ti...C _{ipso} (Å)	Ti–C–C _{ipso} (deg)	interatomic dist (Å)	interatomic angle (deg)
1^+	2.356	80.5	2.481	86.2	H _{py} ...F: 2.239	C–H _{py} ...F: 116.7
2^+	2.360	80.8	2.478	86.1	H _{py} ...F: 2.236	C–H _{py} ...F: 117.0
3^+	2.350	80.1	2.490	86.9	H _{py} ...F: 2.213	C–H _{py} ...F: 141.9
4^+	2.355	80.3	2.507	87.4	H _{py} ...H _{naphthyl} : 2.126	C–H _{py} ...H _{naphthyl} : 98.5

Scheme 3. Gibbs Free Energy Surface for β -Hydrogen Elimination and 2,1-Reinsertion (Pathway c) by INT2a of 4^+ at the B97D Level using LanL2DZ (Ti) and 6-311G(d,p) (Nonmetals) Basis Sets^a



^aRelative energies at 298 K in toluene (kcal/mol) and selected interatomic distances (Å) are given.

propagation reactions by the 4^+ methyl cation, which is a simplified model of 4^+ , was also investigated (Scheme S1 in the Supporting Information). The ΔG_{298}^\ddagger values for the third (in pathway a) and second (in pathway b) C_2H_4 insertions are smaller than the ΔG_{298}^\ddagger values of TS2a and TS2b in pathways a and b, respectively, and such a trend would also be expected for 4^+ . Stabilizing β -agostic ($C_\beta-H_\beta \cdots Ti$) interactions are found for reaction intermediates, such as INT5a and INT5b, in both pathways.

In addition to pathways a and b, attempts have been made to study the viability of alternative reactions and further transformations to give additional active species, as would be anticipated on the basis of the observed multisite behavior of these catalysts. One possible transformation, the rearrangement of an ethylene-assimilated species through β -H elimination (to afford $M-H$ /vinyl species) followed by reinsertion, was spectroscopically observed at ambient temperature by Hessen^{4a} for a cationic $[Ti-CH_2CH_2-arylamine]$ bis(phenolate) complex,⁴⁴ and considered but not detected for the $[N,N,C]$ -Hf system.^{8,9} Coates described the insertion of a pendant vinyl moiety into the metal-C(alkyl) bond of neutral group 4 complexes to afford derivatives bearing tridentate ligands with an ancillary $C(sp^3)$ donor.^{15,16} It is therefore noteworthy that the rearrangement of the ethylene-assimilated species in this work, via β -H elimination and reinsertion to yield a benzylic-type $[Ti-CH(Me)-Ar]$ product, was found to be a feasible pathway (c). Taking 4^+ as an illustrative example (Scheme 3), INT2a can undergo β -H elimination through TS1c ($\Delta G_{298}^\ddagger = 12.0$ kcal/mol relative to $4^+ + C_2H_4$) to form a Ti hydride/vinyl $[CH_2=CH-naphthyl]$ species (INT1c), followed by 2,1-reinsertion via TS2c ($\Delta G_{298}^\ddagger = 17.5$ kcal/mol) to give the $[Ti-CH(Me)-naphthyl]$ complex (INT2c). Alternatively, rather than reinsertion, toluene elimination from INT1c (or chain termination from a polymeryl species to give a saturated chain end) could lead to a dormant or deactivated species. With respect to pathway a,

this β -H elimination and reinsertion pathway would become more accessible at elevated temperatures.

A preliminary study of phenolate substituent effects was performed by comparing 4^+ (^tBu) with 7^+ (CPh₂Me). The respective ΔG_{298}^\ddagger values for TS1a and TS2a are 3.4 and 4.2 kcal/mol (relative to $7^+ + 2C_2H_4$), which are lower than those for 4^+ by 4.4 and 6.4 kcal/mol, respectively, and entirely consistent with its superior polymerization activity at 50 °C (see above). The lower activation energy of TS2a for 7^+ can be correlated with the weaker $Ti \cdots C_{ipso}$ interaction (2.792 Å; $Ti-C-C_{ipso} = 101.5^\circ$) in INT2a, which is longer than that in 4^+ by 0.285 Å. Hence, for pathway a, C_2H_4 insertion into the $Ti-C$ (benzyl) bond for conformers I and II (*anti* to the $[Ti-CH_2CH_2-aryl]$ linkage) proceeds via cleavage of the $Ti \cdots C_{ipso}$ interaction in INT2a, which is weaker and more facile for 7^+ . The dramatic steric influence of the amide substituent in $[N,N,C]$ -Hf catalysts upon polymerization behavior has been noted.¹⁰ Interestingly, $Ti \cdots \pi(Ph)$ coordination^{5,10,45} (2.751 and 2.984 Å) by the CPh₂Me substituent in 7^+ was found to be viable (Figure S4 in the Supporting Information).

Comparisons and General Remarks. In this section, factors affecting activity and rationalization of the effects of the py-adjacent substituent and the formation of multiple catalytic species and the likelihood of different reaction pathways, as well as comparisons with previous work and the $[N,N,C]$ -Hf system, are addressed.

The DFT calculations have provided insight for comparing the py-adjacent substituents and rationalizing the consistently higher activities for σ -naphthyl complexes. (1) The activation barrier (ΔG_{298}^\ddagger) to the ethylene-assimilated species (TS2a) is lowest for the σ -naphthyl derivative (10.6 kcal/mol for 4^+ (benzyl); for comparison, the corresponding barriers (ΔH^\ddagger) for $[N,N,C]$ -Hf alkyl cations (methyl including a $MeB(C_6F_5)_3^-$ anion,^{12,46} *n*-butyl⁸) were calculated to be similar or higher). In addition, a kinetic preference for pathway a (ethylene

assimilation) over **b** (normal propagation), namely $\Delta\Delta G_{298}^\ddagger = \text{TS2b} - \text{TS2a}$ (4.3 kcal/mol for 4^+), is evident for all derivatives except 2^+ (for the Me (^nBu) cation of [N,N,C]-Hf,⁸ $\Delta\Delta H^\ddagger = 7.4$ (2.2) kcal/mol). Therefore, the σ -naphthyl complex is kinetically the most likely to undergo ethylene assimilation for the first insertion (pathway **a**), which proceeds faster than conventional propagation. (2) The activation barrier for pathway **a** is lower than for the conventional propagation pathway **b**, suggesting that the former is dominant and faster and the ethylene-assimilated catalyst is more active. For σ -naphthyl species, this can be explained by the release of $\text{H}_{\text{py}} \cdots \text{H}_{\text{naphthyl}}$ repulsion, while attention is drawn to the more tetrahedral geometry of the Ti center in all ethylene-assimilated structures. Taken together, these points help to explain the enhanced polymerization efficiencies of σ -naphthyl catalysts in comparison with other py-adjacent substituents.

An important aim of this work was to evaluate substituent effects against the (*tert*-butyl)phenolate σ -naphthyl derivative **4**.²⁴ On the basis of DFT calculations, we conclude that a major consequence of a py-adjacent substituent such as the benzo group in **4**–**7** is to facilitate ethylene assimilation (insertion into the Ti–C(σ -aryl) bond) by thermodynamic and kinetic means, as described above. With regard to the role of the phenolate substituent, the ethylene polymerization results indicate that a cumyl substituent can provide suitable protection for the active species and reduce multisite behavior. Improved catalytic performance was realized for the cumyl-phenolate complex **6**, which displays good activity at 50 °C to give polyethylene with an extremely high MW and an M_w/M_n value approaching single-site character.

It is evident from the polymerization and DFT results (and apparent from previous work and related studies) that distinct reaction pathways can transpire for the Ti–[O,N,C(σ -aryl)] system and multiple active sites can be generated, including (i) conventional ethylene insertion into the Ti–C(alkyl) bond and propagation (pathway **b**), and conformers thereof (see **I**–**IV** above), (ii) ethylene-assimilated [Ti–CH₂CH₂–aryl] species from insertion into Ti–C(σ -aryl) bond (pathway **a**), plus subsequent isomerization (pathway **c**) to give [Ti–H/CH₂=CH–aryl] followed by benzylic [Ti–CH(Me)–aryl], and conformers thereof, (iii) degradation or deactivation (arising from e.g. transfer of C₆F₅ moiety from the cocatalyst to Ti,^{11,12,47} reduction,⁴⁸ and ligand abstraction^{35,49} by ⁱBu₃Al), (iv) possible metalation of a phenolate substituent (e.g., Ph⁵ and ⁱPr^{11,14} activation have been reported), (v) additional reaction modes (apart from alkyl abstraction) by the trityl cocatalyst, such as trityl attack at C(σ -aryl) and C(σ -aryl)/isobutyl exchange by ⁱBu₃Al. For (v), the former is considered unlikely on the basis of observations from NMR reactions,³⁶ and the latter would be unexpected (transmetalation generally requires higher activation energies than olefin insertion and is more sensitive to steric factors), but neither of the processes can be discounted (the activation mode and generation of different species, active or otherwise, is dependent upon the nature of the cocatalyst^{11,50,51}). In general, highly active species become more unstable at elevated temperatures as high-energy processes become increasingly populated. Hence, at higher polymerization temperatures, the greater diversity of reaction pathways and active species, each potentially displaying distinctive chain propagation and termination (as well as deactivation) rates, could account for the broad MW distributions of polymers and multisite behavior of these catalysts.

A discussion comparing the polymerization results in this work with related catalysts follows. Under identical conditions, the ethylene polymerization activities for the σ -naphthyl complex **5** are slightly higher than for the σ -phenyl-3,5-bis-(trifluoromethyl) analogue (1.4 and 1.0 kg mmol^{−1} h^{−1} at 50 and 100 °C, respectively),⁵² reaffirming the ability of py-adjacent substituents to increase activity, although the resultant polymers display similarly low M_n values and broad MW distributions. With regard to the [N,N,C]-Hf system, Macchioni proposed¹² that the normal “alkyl-inserted” catalytic species is present in high concentration but displays low or minimal activity, while the olefin-assimilated species forms slowly but undergoes fast propagation (i.e., low concentration but highly active). At first glance, this is broadly consistent with the observations in this work, although clear differences are apparent. For example, DFT calculations suggest that ethylene insertion to form the unassimilated Ti–[O,N,C(σ -aryl)] “alkyl-inserted” cation (pathway **b**) is slow in comparison with the olefin-assimilated species, but this pathway is nevertheless viable and the unassimilated cation should be catalytically active. More generally, Ti–C bonds are weaker and more reactive than Hf–C, and lower activation as well as insertion barriers would be anticipated. The contrasting characteristics of the py-alkyl-amide and py-phenolate chelates (five- and six-membered rings, respectively), and the closer proximity of the amide substituent (compared with phenolate) to the metal center, are also noted.

SUMMARY

A family of group 4 precatalysts supported by [O,N,C] ligands bearing various σ -aryl (py-adjacent) and phenolate substituents has been designed and synthesized. The complexes have been characterized by multinuclear NMR spectroscopy, and η^2 coordination of the benzyl groups was indicated. Ethylene polymerization studies have been undertaken in conjunction with [Ph₃C][B(C₆F₅)₄], and good activities have been observed especially for σ -naphthyl catalysts, which feature a benzo group as the py-adjacent substituent. Replacement of the benzo moiety by one or more F atoms resulted in lower efficiencies.

This work has shown that suitable steric protection afforded by the phenolate substituent can improve catalyst integrity and afford extremely high MW polymers, and narrow MWD (for the cumyl derivative **6**) indicative of close to single-site character is attainable. However, multisite behavior was evident for other catalysts, and attempts to directly observe the active sites using NMR spectroscopy were hampered by their intrinsic instability. Hence, DFT calculations have been performed to probe the polymerization characteristics and especially the initial ethylene insertion and propagation mechanisms, as well as the function of the py-adjacent substituent. Saliiently, these studies revealed several kinetically competitive reaction pathways. In particular, ethylene assimilation (insertion into the Ti–C(σ -aryl) bond) was found to be faster than conventional Ti–C(alkyl) insertion and propagation. In this regard, the benzo py-adjacent substituent is proposed to play an important role in facilitating the formation of the ethylene-assimilated [Ti–CH₂CH₂–naphthyl] species through thermodynamic means (by alleviating steric repulsion to gain stability), as well as by lowering the activation barrier for subsequent ethylene insertion/propagation (by weakening the η^2 -benzyl coordination).

Interestingly, the ethylene-assimilated species exhibits a more tetrahedral Ti center, as a result of the conversion of the *mer*-like [O,N,C(σ -aryl)] ligand into a *fac*-coordinating [O,N,C(C₂H₄-aryl)]

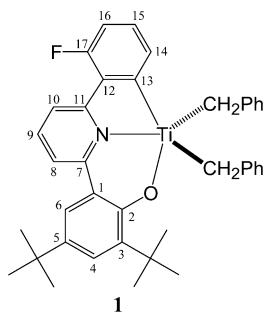
chelate, and subsequent isomerization via β -H elimination and 2,1-reinsertion to give a benzylic-type [Ti-CH(Me)-aryl] complex was shown to be another viable pathway. Overall, the considerable complexity of the Ti-[O,N,C(σ -aryl)] catalyst system has become apparent. The investigations by DFT have indicated the possibility of multiple active sites and further transformations into supplementary active species, each with potentially different chain propagation and termination (as well as degradation) rates, which could account for the observed multisite behavior during polymerization. By considering the insights derived herein, from the polymerization results in conjunction with DFT calculations, future work will focus on controlling the multisite characteristics and the development of well-defined catalysts.

EXPERIMENTAL SECTION

General Considerations. All reactions were performed under a nitrogen atmosphere using standard Schlenk techniques or in a Braun drybox. All solvents were appropriately dried and distilled and then degassed prior to use. ^1H , $^{13}\text{C}\{^1\text{H}\}$ and $^{13}\text{C}[^1\text{H}]$ (referenced to residual solvent peaks), and ^{19}F NMR spectra (external trifluoroacetic acid reference) were recorded at 298 K on Bruker 500 and 400 DRX spectrometers (ppm). Peak assignments were made using DEPT-135 and [$^1\text{H},^1\text{H}$]-COSY, [$^{13}\text{C},^1\text{H}$]-HSQC, and ROESY (plus [$^1\text{H},^{19}\text{F}$]-HMQC for 3) NMR experiments. Elemental analyses were performed on a Vario EL elemental analyzer (Elementar Analysensysteme GmbH). For polymer analysis, gel permeation chromatographs were obtained on a Waters 150CV instrument using polystyrene standards at 140 °C in 1,2-dichlorobenzene. Synthetic procedures for the H_2L^n ligands are given in the Supporting Information. $\text{Ti}(\text{CH}_2\text{Ph})_4$ was prepared according to the published method,⁵³ and the synthesis of 4 was described previously.²⁴

General Synthetic Procedure for 1–3 and 5–7. A solution of H_2L^n (ca. 0.50 mmol) in pentane and diethyl ether (10/2 mL) was added dropwise at -78 °C to $\text{Ti}(\text{CH}_2\text{Ph})_4$ (equimolar to H_2L^n) in pentane and diethyl ether (5/0.5 mL). For H_2L^5 , toluene (5 mL) was used and added to $\text{Ti}(\text{CH}_2\text{Ph})_4$ in pentane (15 mL). The reaction mixture was stirred for 1 h at -78 °C and 12 h at room temperature. Filtration and concentration of the reaction mixture gave a dark red crystalline solid at -25 or -78 °C.

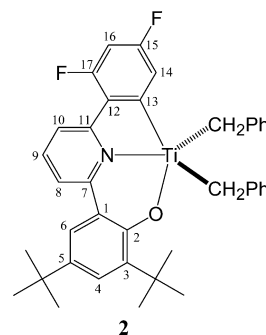
Complex 1.



Yield: 0.25 g, 46%. ^1H NMR (400 MHz, CD_2Cl_2 (aryl resonances overlap significantly in C_6D_6)): δ 1.42 (s, 9H, $5\text{-}^i\text{Bu}$), 1.77 (s, 9H, $3\text{-}^i\text{Bu}$), 3.65 (d, $J = 8.3$ Hz, 2H, CH_2), 3.91 (d, $J = 8.3$ Hz, 2H, CH_2), 6.44–6.50 (m, 6H, o and p -Ph), 6.55 (t, $J = 7.2$ Hz, 4H, m -Ph), 6.91–6.97 (m, 1H, H^{16}), 7.39–7.41 (m, 2H, H^6 and H^{15}), 7.52 (dd, $J = 8.1$ Hz, 1.0 Hz, 1H, H^8), 7.59 (td, $J = 7.9$ Hz, 0.6 Hz, 1H, H^9), 7.61 (d, $J = 2.4$ Hz, 1H, H^4), 7.67 (dd, $J_{\text{H,H}} = 7.9$ Hz, $J_{\text{H,F}} = 2.8$ Hz, 1H, H^{10}), 8.35 (dt, $J = 6.8$ Hz, 1.2 Hz, 1H, H^{14}). ^{13}C NMR (101 MHz, CD_2Cl_2): δ 30.77 (3- CMe_3), 31.62 (5- CMe_3), 34.73 (CMe_3), 35.63 (CMe_3), 92.44 (CH_2 ($J_{\text{C,H}} = 135.0$ Hz)), 115.69 (d, $J = 24.7$ Hz, C^{16}), 120.22 (d, $J = 22.1$ Hz, C^{10}), 122.90, 123.42 (p -Ph), 124.66, 126.93, 127.66 (m -Ph), 130.39 (d, $J = 6.1$ Hz, C^{15}), 130.60 (d, $J = 3.8$ Hz, C^{14}), 130.85 (o -Ph), 139.93, 159.62 (d, $J = 261.5$ Hz, C^{17}); ^4C carbons: 127.07, 136.29, 136.88, 142.64, 156.61, 157.26, 161.01 (d, $J = 7.5$ Hz, C^{12}), 201.80. ^{19}F

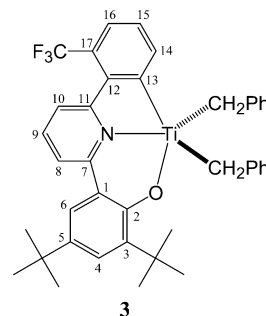
NMR (376 MHz, CD_2Cl_2): δ -114.30 . Anal. Calcd for $\text{C}_{39}\text{H}_{40}\text{NOFTi}$ (605.65): C, 77.34; H, 6.66; N, 2.31. Found: C, 77.33; H, 6.59; N, 2.35.

Complex 2.



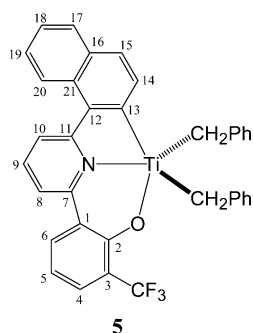
Yield: 0.19 g, 51%. ^1H NMR (400 MHz, C_6D_6): δ 1.35 (s, 9H, $5\text{-}^i\text{Bu}$), 1.80 (s, 9H, $3\text{-}^i\text{Bu}$), 3.88 (d, $J = 8.5$ Hz, 2H, CH_2), 3.98 (d, $J = 8.5$ Hz, 2H, CH_2), 6.41 (t, $J = 7.3$ Hz, 2H, p -Ph), 6.56 (t, $J = 7.7$ Hz, 4H, m -Ph), 6.57–6.62 (m, 1H, H^{16}), 6.69 (d, $J = 7.3$ Hz, 4H, o -Ph), 6.73 (t, $J = 8.1$ Hz, 1H, H^9), 7.05 (d, $J = 7.9$ Hz, 1H, H^8), 7.35 (d, $J = 2.3$ Hz, 1H, H^6), 7.46 (dd, $J_{\text{H,H}} = 8.0$ Hz, $J_{\text{H,F}} = 2.6$ Hz, 1H, H^{10}), 7.69 (d, $J = 2.3$ Hz, 1H, H^4), 8.13 (dd, $J_{\text{H,F}} = 5.6$ Hz, $J_{\text{H,H}} = 2.3$ Hz, 1H, H^{14}). ^{13}C NMR (101 MHz, C_6D_6): δ 30.92 (3- CMe_3), 31.76 (5- CMe_3), 34.67 (CMe_3), 35.74 (CMe_3), 93.68 (CH_2 ($J_{\text{C,H}} = 135.6$ Hz)), 104.02 (virtual t, $J = 27.2$ Hz, C^{16}), 117.01 (dd, $J = 13.7$ Hz, 3.4 Hz, C^{14}), 119.75 (d, $J = 22.0$ Hz, C^{10}), 122.30, 124.12 (p -Ph), 124.68, 126.88, 128.01 (m -Ph), 131.56 (o -Ph), 139.77, 160.20 (dd, $J = 266.3$, 8.0 Hz, C^{17}), 163.16 (dd, $J = 262.0$, 7.6 Hz, C^{15}); ^4C carbons: 125.20, 136.22, 136.63, 142.73, 156.81, 157.31, 160.51 (d, $J = 7.9$ Hz, C^{12}), 202.48 (d, $J = 6.7$ Hz). ^{19}F NMR (376 MHz, C_6D_6): δ -108.47 (d, $J = 11.3$ Hz), -109.17 (d, $J = 11.3$ Hz). Anal. Calcd for $\text{C}_{39}\text{H}_{40}\text{NOFTi}$ (623.64): C, 75.11; H, 6.30; N, 2.25. Found: C, 75.14; H, 6.13; N, 2.30.

Complex 3.



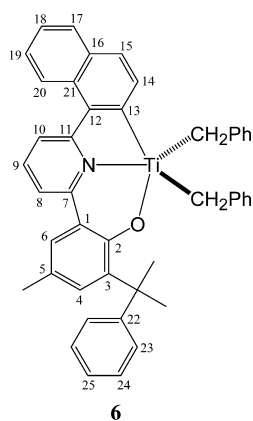
Yield: 0.24 g, 78%. ^1H NMR (400 MHz, C_6D_6): δ 1.35 (s, 9H, $5\text{-}^i\text{Bu}$), 1.84 (s, 9H, $3\text{-}^i\text{Bu}$), 3.94 (d, $J = 8.4$ Hz, 2H, CH_2), 4.08 (d, $J = 8.4$ Hz, 2H, CH_2), 6.38 (t, $J = 7.4$ Hz, 2H, p -Ph), 6.52 (t, $J = 7.8$ Hz, 4H, m -Ph), 6.62 (d, $J = 7.2$ Hz, 4H, o -Ph), 6.73 (t, $J = 8.0$ Hz, 1H, H^9), 7.07 (d, $J = 8.0$ Hz, 1H, H^8), 7.14 (t, $J = 7.6$ Hz, 1H, H^{15}), 7.25 (d, $J = 8.0$ Hz, 1H, H^{10}), 7.34 (d, $J = 2.4$ Hz, 1H, H^6), 7.52 (d, $J = 7.6$ Hz, 1H, H^{16}), 7.73 (d, $J = 2.4$ Hz, 1H, H^4), 8.61 (d, $J = 6.8$ Hz, 1H, H^{14}). ^{13}C NMR (101 MHz, C_6D_6): δ 31.53 (3- CMe_3), 32.31 (5- CMe_3), 35.26 (CMe_3), 36.32 (CMe_3), 93.27 (CH_2 ($J_{\text{C,H}} = 135.8$ Hz)), 121.64 (q, $J = 7.0$ Hz, C^{10}), 123.45 (C^8), 124.56 (p -Ph), 125.57 (C^6), 127.34 (C^4), 127.95 (q, $J = 6.0$ Hz, C^{16}), 128.18 (C^{15}), 128.49 (m -Ph), 131.96 (o -Ph), 138.86 (C^{14}), 139.67 (C^9), 142.49 (m, CF_3); ^4C carbons: 126.26, 129.90, 136.73, 137.38, 143.33, 157.85, 158.86, 163.62, 202.77. ^{19}F NMR (376 MHz, C_6D_6): δ -54.71 . Anal. Calcd for $\text{C}_{40}\text{H}_{40}\text{NOF}_3\text{Ti}$ (655.66): C, 73.28; H, 6.15; N, 2.14. Found: C, 73.49; H, 6.19; N, 2.01.

Complex 5.



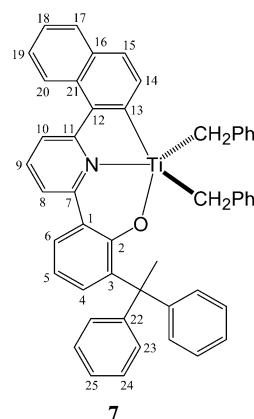
Yield: 0.13 g, 40%. $^1\text{H NMR}$ (400 MHz, C_6D_6): δ 4.05 (d, $J = 8.2$ Hz, 2H, CH_2), 4.15 (d, $J = 8.2$ Hz, 2H, CH_2), 6.33 (t, $J = 7.2$ Hz, 2H, $p\text{-Ph}$), 6.45 (t, $J = 7.4$ Hz, 4H, $m\text{-Ph}$), 6.54 (t, $J = 7.2$ Hz, 1H, H^5), 6.67 (m, 2H, H^8 and H^9), 6.76 (d, $J = 7.6$ Hz, 4H, $o\text{-Ph}$), 7.08–7.13 (m, 2H, H^6 and H^{10}), 7.29 (m, 2H, H^{18} and H^{19}), 7.56 (d, $J = 7.2$ Hz, 1H, H^4), 7.66 (d, $J = 7.6$ Hz, 1H, H^{15}), 7.75 (d, $J = 8.0$ Hz, 1H, H^{17}), 8.04 (d, $J = 7.6$ Hz, 1H, H^{20}), 8.67 (d, $J = 8.0$ Hz, 1H, H^{14}). $^{13}\text{C NMR}$ (101 MHz, C_6D_6): δ 96.98 (CH_2 ($^1J_{\text{C,H}} = 137.4$ Hz)), 119.67 (C^5), 121.49 (C^8), 121.65 (C^{10}), 124.64 ($p\text{-Ph}$), 125.12 (C^{20}), 126.44, 127.36, 128.41 ($m\text{-Ph}$), 128.62 (C^{15}), 129.76 (m, CF_3), 129.90 (C^4), 130.39 (C^{17}), 132.50 ($o\text{-Ph}$), 133.33 (C^6 and C^{14}), 139.52 (C^9); 4° carbons: 119.67, 135.88, 136.86, 139.94, 156.80, 158.99, 165.52, 204.32. $^{19}\text{F NMR}$ (376 MHz, C_6D_6): δ -61.50. Anal. Calcd for $\text{C}_{36}\text{H}_{26}\text{NOF}_3\text{Ti}$ (593.50): C, 72.85; H, 4.42; N, 2.36. Found: C, 72.93; H, 4.79; N, 2.04.

Complex 6.



Yield: 0.10 g, 27%. $^1\text{H NMR}$ (400 MHz, C_6D_6): δ 1.99 (s, 6H, CMe_2), 2.36 (s, 3H, ArMe), 3.42 (d, $J = 8.0$ Hz, 2H, CH_2), 4.09 (d, $J = 8.0$ Hz, 2H, CH_2), 6.30 (t, $J = 7.2$ Hz, 2H, $p\text{-CH}_2\text{Ph}$), 6.34 (d, $J = 7.2$ Hz, 4H, $o\text{-CH}_2\text{Ph}$), 6.41 (t, $J = 7.4$ Hz, 4H, $m\text{-CH}_2\text{Ph}$), 6.64 (t, $J = 8.0$ Hz, 1H, H^9), 6.93 (d, $J = 8.0$ Hz, 1H, H^8), 7.00–7.03 (m, 2H, H^{10} and H^{25}), 7.21 (m, 1H, H^6), 7.23–7.29 (m, 4H, H^{18} , H^{19} and H^{24}), 7.56–7.58 (m, 3H, H^4 and H^{23}), 7.63 (d, $J = 7.6$ Hz, 1H, H^{15}), 7.72 (d, $J = 8.4$ Hz, 1H, H^{17}), 7.98 (d, $J = 8.0$ Hz, 1H, H^{20}), 8.66 (d, $J = 7.6$ Hz, 1H, H^{14}). $^{13}\text{C NMR}$ (101 MHz, C_6D_6): δ 22.05 (Me), 31.39 (CMe_2), 43.07 (CMe_2), 94.33 (CH_2 ($^1J_{\text{C,H}} = 135.3$ Hz)), 120.91 (C^{10}), 121.73 (C^8), 124.01 ($p\text{-Ph}$), 125.09 (C^{20}), 125.95, 126.78, 126.83 (C^{23}), 126.93, 128.03 ($m\text{-Ph}$), 128.19 (C^{15}), 129.07 (C^6), 129.31 (C^{24}), 130.16 (C^{17}), 131.40 (C^4), 131.87 ($o\text{-Ph}$), 133.47 (C^{14}), 139.04 (C^9); 4° carbons: 129.26, 129.83, 135.73, 137.41, 138.33, 139.74, 152.01, 157.68, 158.51, 165.30, 204.29. Anal. Calcd for $\text{C}_{45}\text{H}_{39}\text{NOTi}$ (657.71): C, 82.18; H, 5.98; N, 2.13. Found: C, 82.43; H, 5.69; N, 2.24.

Complex 7.



Yield: 0.09 g, 28%. $^1\text{H NMR}$ (400 MHz, C_6D_6): δ 2.92 (s, 3H, Me), 3.36 (d, $J = 8.0$ Hz, 2H, CH_2), 4.01 (d, $J = 8.0$ Hz, 2H, CH_2), 6.36 (m, 2H, $p\text{-CH}_2\text{Ph}$), 6.41–6.49 (m, 8H, $o\text{-}$ and $m\text{-CH}_2\text{Ph}$), 6.64 (t, $J = 7.9$ Hz, 1H, H^9), 6.71 (t, $J = 7.5$ Hz, 1H, H^5), 6.94 (d, $J = 7.9$ Hz, 1H, H^8), 7.01–7.08 (m, 3H, H^{10} and H^{25}), 7.16–7.33 (m, 7H, H^6 , H^{18} , H^{19} and H^{24}), 7.40 (d, $J = 7.3$ Hz, 5H, H^4 and H^{23}), 7.61 (d, $J = 7.6$ Hz, 1H, H^{15}), 7.72 (m, 1H, H^{17}), 7.99 (m, 1H, H^{20}), 8.59 (d, $J = 7.6$ Hz, 1H, H^{14}). $^{13}\text{C NMR}$ (101 MHz, C_6D_6): δ 30.00 (CMe), 53.42 (CMe), 94.54 (CH_2 ($^1J_{\text{C,H}} = 135.3$ Hz)), 120.24 (C^5), 121.01 (C^{10}), 121.97 (C^8), 124.19 ($p\text{-CH}_2\text{Ph}$), 125.12 (C^{20}), 125.99, 126.97, 127.16 (C^{25}), 128.19 ($m\text{-CH}_2\text{Ph}$), 128.91 (C^{15}), 129.08 (C^{23}), 129.22 (C^4), 129.65 (C^{24}), 130.16 (C^{17}), 131.87 ($o\text{-CH}_2\text{Ph}$), 133.24 (C^6), 134.76 (C^{14}), 139.18 (C^9); 4° carbons: 129.64, 129.81, 135.74, 137.55, 138.53, 139.48, 149.76, 158.59, 160.12, 165.30, 204.62. Anal. Calcd for $\text{C}_{49}\text{H}_{39}\text{NOTi}$ (705.71): C, 83.39; H, 5.57; N, 1.98. Found: C, 83.51; H, 5.36; N, 2.22.

Polymerization Procedure. Ethylene polymerization tests using $[\text{Ph}_3\text{C}][\text{B}(\text{C}_6\text{F}_5)_4]$ as cocatalyst were carried out in toluene in a 10 mL glass reactor equipped with a paddlelike stirrer. Toluene (3.5 mL) was introduced into the nitrogen-purged reactor and vigorously stirred (600 rpm). The toluene was thermostated to the required temperature, and the ethylene gas feed (7 atm) was then started and maintained during the experiment. After 15 min, polymerization was initiated by consecutively adding toluene solutions of tBu_3Al , cocatalyst, and catalyst into the reactor (total volume 5.0 mL) with stirring. After the prescribed time, isobutyl alcohol (0.5 mL) was added to terminate the polymerization, and the ethylene feed was stopped. The polymer was collected by filtration, washed with methanol (20 mL) and concentrated HCl (2 mL), and dried in vacuo at 80°C for 10 h. Errors for the activity values are estimated to be $\pm 10\%$, on the basis of previous polymerization tests using the same experimental procedure and reactor.

■ ASSOCIATED CONTENT

S Supporting Information

Text, figures, and tables giving experimental details and characterization data for H_2L^{1-7} , selected NMR data for 1–7, GPC traces, and additional results for DFT calculations. This material is available free of charge via the Internet at <http://pubs.acs.org>.

■ AUTHOR INFORMATION

Corresponding Author

*E-mail: mwcwan@cityu.edu.hk (M.C.W.C.); kaichung@cityu.edu.hk (K.-C.L.).

Notes

The authors declare no competing financial interest.

ACKNOWLEDGMENTS

The work described in this paper was supported by the Research Grants Council of the Hong Kong SAR, China (CityU 100307); the theoretical work was supported by a Strategic Research Grant from City University of Hong Kong (Project No. 7002616). We are grateful to Dr. Ka-Ho Tam (City University of Hong Kong) and Hiromu Kaneyoshi (Mitsui Chemicals, Inc.) for assistance in synthetic and polymerization studies, respectively.

REFERENCES

- (1) (a) Resconi, L.; Chadwick, J. C.; Cavallo, L. In *Comprehensive Organometallic Chemistry III*; Crabtree, R. H., Mingos, D. M. P., Bochmann, M., Eds.; Elsevier: Oxford, U.K., 2007; Vol. 4, pp 1005–1166. (b) Fujita, T.; Makio, H. In *Comprehensive Organometallic Chemistry III*; Crabtree, R. H., Mingos, D. M. P., Hiyama, T., Eds.; Elsevier: Oxford, U.K., 2007; Vol. 11, pp 691–734. (c) Gibson, V. C.; Spitzmesser, S. K. *Chem. Rev.* **2003**, *103*, 283.
- (2) (a) Pindado, G. J.; Thornton-Pett, M.; Bouwkamp, M.; Meetsma, A.; Hessen, B.; Bochmann, M. *Angew. Chem., Int. Ed. Engl.* **1997**, *36*, 2358. (b) Skoog, S. J.; Mateo, C.; Lavoie, G. G.; Hollander, F. J.; Bergman, R. G. *Organometallics* **2000**, *19*, 1406. (c) Karl, J.; Erker, G.; Fröhlich, R. *J. Am. Chem. Soc.* **1997**, *119*, 11165. (d) Said, M.; Thornton-Pett, M.; Bochmann, M. *Dalton Trans.* **2001**, 2844.
- (3) Bouwkamp, M.; van Leusen, D.; Meetsma, A.; Hessen, B. *Organometallics* **1998**, *17*, 3645.
- (4) (a) Gielens, E. E. C. G.; Dijkstra, T. W.; Berno, P.; Meetsma, A.; Hessen, B.; Teuben, J. H. *J. Organomet. Chem.* **1999**, *591*, 88. (b) For related insertion chemistry of zirconocene complexes, see: Jordan, R. F.; Taylor, D. F.; Baenziger, N. C. *Organometallics* **1990**, *9*, 1546.
- (5) Deckers, P. J. W.; Hessen, B. *Organometallics* **2002**, *21*, 5564.
- (6) Shao, P.; Gendron, R. A. L.; Berg, D. J.; Bushnell, G. W. *Organometallics* **2000**, *19*, 509.
- (7) (a) Boussie, T. R.; Diamond, G. M.; Goh, C.; Hall, K. A.; LaPointe, A. M.; Leclerc, M. K.; Murphy, V.; Shoemaker, J. A. W.; Turner, H.; Rosen, R. K.; Stevens, J. C.; Alfano, F.; Busico, V.; Cipullo, R.; Talarico, G. *Angew. Chem., Int. Ed.* **2006**, *45*, 3278. (b) Boussie, T. R.; Diamond, G. M.; Goh, C.; Hall, K. A.; LaPointe, A. M.; Leclerc, M. K.; Lund, C.; Murphy, V. PCT Int. Appl. WO 038628, 2002.
- (8) Froese, R. D. J.; Hustad, P. D.; Kuhlman, R. L.; Wenzel, T. T. *J. Am. Chem. Soc.* **2007**, *129*, 7831.
- (9) Busico, V.; Cipullo, R.; Pellecchia, R.; Rongo, L.; Talarico, G.; Macchioni, A.; Zuccaccia, C.; Froese, R. D. J.; Hustad, P. D. *Macromolecules* **2009**, *42*, 4369.
- (10) Domski, G. J.; Lobkovsky, E. B.; Coates, G. W. *Macromolecules* **2007**, *40*, 3510.
- (11) Zuccaccia, C.; Macchioni, A.; Busico, V.; Cipullo, R.; Talarico, G.; Alfano, F.; Boone, H. W.; Frazier, K. A.; Hustad, P. D.; Stevens, J. C.; Vosejpk, P. C.; Abboud, K. A. *J. Am. Chem. Soc.* **2008**, *130*, 10354.
- (12) Zuccaccia, C.; Busico, V.; Cipullo, R.; Talarico, G.; Froese, R. D. J.; Vosejpk, P. C.; Hustad, P. D.; Macchioni, A. *Organometallics* **2009**, *28*, 5445.
- (13) Frazier, K. A.; Froese, R. D.; He, Y.; Klosin, J.; Theriault, C. N.; Vosejpk, P. C.; Zhou, Z.; Abboud, K. A. *Organometallics* **2011**, *30*, 3318.
- (14) Luconi, L.; Rossin, A.; Tuci, G.; Tritto, I.; Boggioni, L.; Klosin, J.; Theriault, C. N.; Giambastiani, G. *Chem. Eur. J.* **2012**, *18*, 671.
- (15) Domski, G. J.; Edson, J. B.; Keresztes, I.; Lobkovsky, E. B.; Coates, G. W. *Chem. Commun.* **2008**, 6137.
- (16) Edson, J. B.; Keresztes, I.; Lobkovsky, E. B.; Coates, G. W. *ChemCatChem* **2009**, *1*, 122.
- (17) Tsurugi, H.; Yamamoto, K.; Mashima, K. *J. Am. Chem. Soc.* **2011**, *133*, 732.
- (18) Kui, S. C. F.; Zhu, N.; Chan, M. C. W. *Angew. Chem., Int. Ed.* **2003**, *42*, 1628.
- (19) Chan, M. C. W.; Kui, S. C. F.; Cole, J. M.; McIntyre, G. J.; Matsui, S.; Zhu, N.; Tam, K. H. *Chem. Eur. J.* **2006**, *12*, 2607.
- (20) (a) Chan, M. C. W. *Chem. Asian J.* **2008**, *3*, 18. (b) Mitani, M.; Nakano, T.; Fujita, T. *Chem. Eur. J.* **2003**, *9*, 2396.
- (21) Popeney, C. S.; Rheingold, A. L.; Guan, Z. *Organometallics* **2009**, *28*, 4452.
- (22) Weberski, M. P., Jr.; Chen, C.; Delferro, M.; Zuccaccia, C.; Macchioni, A.; Marks, T. J. *Organometallics* **2012**, *31*, 3773.
- (23) Tam, K. H.; Lo, J. C. Y.; Guo, Z.; Chan, M. C. W. *J. Organomet. Chem.* **2007**, *692*, 4750.
- (24) Tam, K. H.; Chan, M. C. W.; Kaneyoshi, H.; Makio, H.; Zhu, N. *Organometallics* **2009**, *28*, 5877.
- (25) Since “olefin-inserted” can also refer to the normal chain propagation process, the term “olefin-assimilated” is preferred to unambiguously describe the modified $[M-C_2H_3R-aryl]$ species arising from olefin insertion into the $M-C(sp^2)$ bond of a chelating σ -aryl ligand.
- (26) (a) Razavi, A.; Atwood, J. L. *J. Organomet. Chem.* **1996**, *520*, 115. (b) Dreier, T.; Erker, G. *Isr. J. Chem.* **2002**, *42*, 343. (c) Zhang, Y.; Reeder, E. K.; Keaton, R. J.; Sita, L. R. *Organometallics* **2004**, *23*, 3512. (d) Bastero, A.; Göttker-Schnetmann, I.; Röhr, C.; Mecking, S. *Adv. Synth. Catal.* **2007**, *349*, 2307.
- (27) Wang, B. *Coord. Chem. Rev.* **2006**, *250*, 242.
- (28) For example, see: (a) Hu, P.; Qiao, Y.-L.; Wang, J.-Q.; Jin, G.-X. *Organometallics* **2012**, *31*, 3241. (b) Huang, W.; Zhang, W.; Sun, W.-H.; Wang, L.; Redshaw, C. *Catal. Sci. Technol.* **2012**, *2*, 2090. (c) Hu, P.; Wang, F.; Jin, G.-X. *Organometallics* **2011**, *30*, 1008. (d) Huang, W.; Sun, W.-H.; Redshaw, C. *Dalton Trans.* **2011**, *40*, 6802. (e) Zhang, J.; Wang, X.; Jin, G.-X. *Coord. Chem. Rev.* **2006**, *250*, 95.
- (29) Silva, A. M. S.; Almeida, L. M. P. M.; Cavaleiro, J. A. S.; Foces-Foces, C.; Llamas-Saiz, A. L.; Fontenas, C.; Jagerovic, N.; Elguero, J. *Tetrahedron* **1997**, *53*, 11645.
- (30) Chan, M. C. W.; Tam, K.-H.; Pui, Y.-L.; Zhu, N. *Dalton Trans.* **2002**, 3085.
- (31) (a) Latesky, S. L.; McMullen, A. K.; Niccolai, G. P.; Rothwell, I. P.; Huffman, J. C. *Organometallics* **1985**, *4*, 902. (b) Jordan, R. F.; LaPointe, R. E.; Baenziger, N.; Hinch, G. D. *Organometallics* **1990**, *9*, 1539. (c) Bochmann, M.; Lancaster, S. J. *Organometallics* **1993**, *12*, 633. (d) Bei, X.; Swenson, D. C.; Jordan, R. F. *Organometallics* **1997**, *16*, 3282.
- (32) The “syn, anti” arrangement of bis(benzyl) moieties is typical for related post-metallocenes displaying trigonal-bipyramidal geometry, e.g.: Tshuva, E. Y.; Goldberg, I.; Kol, M.; Goldschmidt, Z. *Organometallics* **2001**, *20*, 3017.
- (33) Himes, R. A.; Fanwick, P. E.; Rothwell, I. P. *Chem. Commun.* **2003**, 18.
- (34) (a) Tsukahara, T.; Swenson, D. C.; Jordan, R. F. *Organometallics* **1997**, *16*, 3303. (b) O'Connor, P. E.; Morrison, D. J.; Steeves, S.; Burrage, K.; Berg, D. J. *Organometallics* **2001**, *20*, 1153. (c) Schrock, R. R.; Adamchuk, J.; Ruhland, K.; Lopez, L. P. H. *Organometallics* **2003**, *22*, 5079. (d) Lavanant, L.; Chou, T.-Y.; Chi, Y.; Lehmann, C. W.; Toupet, L.; Carpentier, J.-F. *Organometallics* **2004**, *23*, 5450. (e) Merle, P. G.; Chéron, V.; Hagen, H.; Lutz, M.; Spek, A. L.; Deelman, B.-J.; van Koten, G. *Organometallics* **2005**, *24*, 1620. (f) Sergeeva, E.; Kopilov, J.; Goldberg, I.; Kol, M. *Inorg. Chem.* **2009**, *48*, 8075. (g) Annunziata, L.; Pappalardo, D.; Tedesco, C.; Pellecchia, C. *Organometallics* **2009**, *28*, 688.
- (35) Matsui, S.; Mitani, M.; Saito, J.; Tohi, Y.; Makio, H.; Matsukawa, N.; Takagi, Y.; Tsuru, K.; Nitabar, M.; Nakano, T.; Tanaka, H.; Kashiwa, N.; Fujita, T. *J. Am. Chem. Soc.* **2001**, *123*, 6847.
- (36) Characterization of the products from treatment of the bis(benzyl) complexes with $[Ph_3C][B(C_6F_5)_4]$ in an NMR tube was attempted in various solvents (d_5 -bromobenzene, CD_2Cl_2 , d_8 -toluene; plus drops of d_8 -THF) at +20 and –20 °C. Although complicated mixtures were obtained, the formation of significant amounts of Ph_3CCH_2Ph was observed, providing support for benzyl abstraction and generation of the benzyl cationic species (and against trityl attack at the C(σ -aryl) atom).
- (37) Grimme, S. *J. Comput. Chem.* **2006**, *27*, 1787.

(38) (a) Hay, P. J.; Wadt, W. R. *J. Chem. Phys.* **1985**, *82*, 270. (b) Hay, P. J.; Wadt, W. R. *J. Chem. Phys.* **1985**, *82*, 284. (c) Wadt, W. R.; Hay, P. J. *J. Chem. Phys.* **1985**, *82*, 299.

(39) (a) Miertuš, S.; Scrocco, E.; Tomasi, J. *Chem. Phys.* **1981**, *55*, 117. (b) Miertuš, S.; Tomasi, J. *Chem. Phys.* **1982**, *65*, 239.

(40) Frisch, M. J. et al. *Gaussian 09, revision B.1*; Gaussian, Inc., Wallingford, CT, 2009.

(41) For DFT calculations discussed in this work where multiple conformers are possible, only the lowest energy conformer is quoted and discussed.

(42) The respective $\Delta G_{323}^{\ddagger}$ values for **TS2a/TS2b** of **1⁺** (15.2/14.6 kcal/mol), **2⁺** (16.6/14.5 kcal/mol), **3⁺** (12.7/14.7 kcal/mol), and **4⁺** (12.6/16.0 kcal/mol) are higher than the corresponding $\Delta G_{298}^{\ddagger}$ values by ca. 2.0/1.0 kcal/mol, and hence the same reactivity trend is evident.

(43) (a) Thalladi, V. R.; Weiss, H.-C.; Bläser, D.; Boese, R.; Nangia, A.; Desiraju, G. R. *J. Am. Chem. Soc.* **1998**, *120*, 8702. (b) Haufe, G.; Rosen, T. C.; Meyer, O. G. J.; Fröhlich, R.; Rissanen, K. *J. Fluorine Chem.* **2002**, *114*, 189. (c) Parsch, J.; Engels, J. W. *J. Am. Chem. Soc.* **2002**, *124*, 5664. (d) Watt, S. W.; Dai, C.; Scott, A. J.; Burke, J. M.; Thomas, R. L.; Collings, J. C.; Viney, C.; Clegg, W.; Marder, T. B. *Angew. Chem., Int. Ed.* **2004**, *43*, 3061. (e) Anzahaee, M. Y.; Watts, J. K.; Alla, N. R.; Nicholson, A. W.; Damha, M. J. *J. Am. Chem. Soc.* **2011**, *133*, 728. (f) Prakash, G. K. S.; Wang, F.; Rahm, M.; Shen, J.; Ni, C.; Haiges, R.; Olah, G. A. *Angew. Chem., Int. Ed.* **2011**, *50*, 11761. Organometallic example: (g) Fekl, U.; van Eldik, R.; Lovell, S.; Goldberg, K. I. *Organometallics* **2000**, *19*, 3535.

(44) In comparison with amine-based ligands, the greater rigidity of the pyridine moiety in the present work should increase the activation barrier for this rearrangement reaction.

(45) Saßmannshausen, J.; Powell, A. K.; Anson, C. E.; Wocadlo, S.; Bochmann, M. *J. Organomet. Chem.* **1999**, *592*, 84.

(46) The authors proposed that in the absence of the counterion the calculated barriers are artificially low, and therefore it would be appropriate to compare activation barriers to indicate selectivity only.

(47) (a) Yang, X. M.; Stern, C. L.; Marks, T. J. *J. Am. Chem. Soc.* **1994**, *116*, 10015. (b) Scollard, J. D.; McConville, D. H.; Rettig, S. J. *Organometallics* **1997**, *16*, 1810. (c) Phomphrai, K.; Fenwick, A. E.; Sharma, S.; Fanwick, P. E.; Caruthers, J. M.; Delgass, W. N.; Abu-Omar, M. M.; Rothwell, I. P. *Organometallics* **2006**, *25*, 214.

(48) Knight, P. D.; Clarkson, G.; Hammond, M. L.; Kimberley, B. S.; Scott, P. *J. Organomet. Chem.* **2005**, *690*, 5125.

(49) Makio, H.; Fujita, T. *Macromol. Symp.* **2004**, *213*, 221.

(50) Chen, E. Y.-X.; Marks, T. J. *Chem. Rev.* **2000**, *100*, 1391.

(51) Bochmann, M. *Organometallics* **2010**, *29*, 4711.

(52) Liu, C.-C.; So, L.-C.; Lo, J. C. Y.; Chan, M. C. W.; Kaneyoshi, H.; Makio, H. *Organometallics* **2012**, *31*, 5274.

(53) Zucchini, U.; Albizzati, E.; Giannini, U. *J. Organomet. Chem.* **1971**, *26*, 357.